The effect of a vertical lapse rate of temperature on the spiral flow of a fluid in a heated rotating cylinder

By G. N. LANCE
Computation Laboratory, University of Southampton

(*Received* 8 *October* 1957)

SUMMARY

Experiments have been performed with a viscous fluid contained in a rotating cylinder heated from below. Previous theoretical explanations of the flow patterns obtained in these experiments assumed that the convective terms in the heat transfer equation were negligible. The present paper gives a treatment which includes one of these convective terms. The results confirm the physical reasoning that, when the lapse rate is positive, the stability is increased and that the motion is therefore decreased.

1. INTRODUCTION

Many experiments have been performed with a fluid in a rotating dish-pan which is heated from below. The case of a shallow fluid has been covered very fully by Fultz (1951, 1956). Several authors have put forward theories which attempt to explain the results. Davies (1953) used a theory which neglected convective terms in the heat transfer equation, whereas Kuo (1954, 1955, 1956) included both horizontal and vertical temperature gradients, but both these theories needed, for their success, the assumption of a shallow fluid.

Experiments with deep fluids have been described by Fultz (1956). Skeib (1953) performed experiments with a value of a, which is effectively a depth parameter (see § 3), very nearly equal to unity. Unity is the value of a which is used, in this paper, to obtain the curves shown in figures 1–3. Davies's theory was extended to cover larger depths by Lance & Deland (1955) but they neglected the convective terms in the heat transfer equation (in the present paper this reference will be referred to as I).

In the dish-pan experiments the fluid was heated near the circumference of the base of the dish-pan and cooled near the axis of rotation. All the theories so far put forward have used the method of small perturbations, the perturbations being superimposed on a steady state of rotation without heating and at constant basic pressure, density and temperature. Previous theories, with the exception of Kuo's (1954), have assumed that the vertical temperature lapse rate was zero but the experimental results have shown that in fact the temperature varies in a manner which is very nearly a linear function of height. The purpose of the present paper is to determine the effect of this vertical lapse rate and to see whether the flow patterns previously given in I are greatly altered by the lapse rate.

2. The equations of motion

The notation used here is the same as that employed in I, where the equations of motion were presented in full. If it is assumed that the motion is axially symmetric and that a steady state has been reached, then the equations can be written, using cylindrical polar coordinates (r, θ, z), in the following form:

$$\rho_1\left(\frac{Du_1}{Dt} - \frac{v_1^2}{r}\right) = -\frac{\partial p_1}{\partial r} + \mu\left(\nabla^2 u_1 - \frac{u_1}{r^2}\right) + \tfrac{1}{3}\mu\frac{\partial \psi_1}{\partial r}, \tag{1}$$

$$\rho_1\left(\frac{Dv_1}{Dt} + \frac{u_1 v_1}{r}\right) = \mu\left(\nabla^2 v_1 - \frac{v_1}{r^2}\right), \tag{2}$$

$$\rho_1\frac{Dw_1}{Dt} = -\frac{\partial p_1}{\partial z} - g\rho_1 + \mu\nabla^2 w_1 + \tfrac{1}{3}\mu\frac{\partial \psi_1}{\partial z}, \tag{3}$$

$$\frac{D\rho_1}{Dt} = -\rho_1\psi_1, \tag{4}$$

$$\rho_1 = \rho_0 - \alpha(T_1 - T_0), \tag{5}$$

$$\rho_1 J c_v \frac{DT_1}{Dt} = Jk\nabla^2 T_1 + \Phi_1 + p_1\psi_1. \tag{6}$$

In the above six equations, u_1, v_1, w_1 are the components of fluid velocity in the directions of r, θ and z increasing, respectively, relative to an axis system fixed in space with the origin at the centre of the base of the dish-pan. The pressure is denoted by p_1 and the density by ρ_1; μ is the coefficient of viscosity, α is the reciprocal of the coefficient of cubical expansion, J is the mechanical equivalent of heat, c_v is the specific heat at constant volume, k is the thermometric conductivity and Φ_1 is the viscous dissipation function. Also,

$$\frac{D}{Dt} \equiv u_1\frac{\partial}{\partial r} + w_1\frac{\partial}{\partial z}, \qquad \nabla^2 \equiv \frac{\partial^2}{\partial r^2} + \frac{1}{r}\frac{\partial}{\partial r} + \frac{\partial^2}{\partial z^2},$$

and

$$\psi_1 \equiv \frac{\partial u_1}{\partial r} + \frac{u_1}{r} + \frac{\partial w_1}{\partial z}.$$

When the liquid is not heated, rotation of the cylinder causes solid rotation of the fluid and, if heat is supplied, the departures from the state of solid rotation will be small. Thus, if Ω is the angular velocity of the cylinder, we write

$$\left.\begin{aligned} u_1 = u, \qquad v_1 = \Omega r + v, \qquad w_1 = w, \qquad \rho_1 = \rho_0 + \rho, \\ p_1 = p_0 + p, \qquad T_1 = T_0 + T. \end{aligned}\right\} \tag{7}$$

The symbols without suffixes are the six perturbation quantities which determine the departure from the state of solid rotation. It was shown in I that, if attention is confined to slow rates of rotation (as in the experiments), the upper surface of the liquid is approximately the horizontal plane $z = h$, where h is the depth of the fluid.

When the expressions (7) are substituted into (1) to (6), the following equations are obtained for the perturbation variables:

$$-2\Omega\rho_0 v = -\partial p/\partial r + \mu(\nabla^2 u - u/r^2), \tag{8}$$

$$+2\Omega\rho_0 u = \mu(\nabla^2 v - v/r^2), \tag{9}$$

$$-\partial p/\partial z - g\rho + \mu\nabla^2 w = 0, \tag{10}$$

$$r\psi_1 \equiv \partial(ru)/\partial r + \partial(rw)/\partial z = 0, \tag{11}$$

$$\rho = -\alpha T, \tag{12}$$

$$\nabla^2 T = (\rho c_v/k) DT/Dt, \tag{13}$$

where all non-linear terms have been neglected. Now, for the purposes of the present paper, it is assumed that $\partial T_0/\partial z \equiv \Theta = \text{const.}$, so that (13) reduces to

$$\nabla^2 T = (\rho c_v/k)\Theta w, \tag{14}$$

the work of I simply took $\Theta = 0$.

The term containing $\partial T_0/\partial r$ has been omitted and there is, in fact, no real justification for such an omission; however, it does enable the variables r and z to be separated and in this way the equations can be reduced to ordinary differential equations (see (17) to (20) below). Moreover, such a procedure has the advantage that the effect of only one advection term may be obtained and their relative importance may be determined. Finally, if the density is eliminated from (10) and (12) it is found that

$$-\partial p/\partial z + g\alpha T + \mu\nabla^2 w = 0. \tag{15}$$

3. Reduction of the equations to a system of ordinary differential equations

It was shown in I that the variables r and z can be separated by the substitutions

$$\left.\begin{aligned} T(r,z) &= T_1(z)J_0(\beta r), \\ u(r,z) &= U_1(z)J_1(\beta r), \\ v(r,z) &= V_1(z)J_1(\beta r), \\ w(r,z) &= W_1(z)J_0(\beta r), \\ p(r,z) &= P_1(z)J_0(\beta r), \\ \rho(r,z) &= \Pi(z)J_0(\beta r), \end{aligned}\right\} \tag{16}$$

where βr_0 is a zero of $J_1(\beta r_0) = 0$ and r_0 is the radius of the dish-pan.

It is only possible to retain the vertical lapse rate in (14) because the r variation of both T and w is of the form $J_0(\beta r)$. If the form were not the same for both these variables the r coordinate would not cancel from this equation and the system of partial differential equations could not be reduced to a system of ordinary differential equations. As in I, all the quantities may be written in non-dimensional form and the pressure can be eliminated from (8) and (10). The final system of equations is

$$U''' - a^2U' + 2RV' + aW'' - a^3W + aT = 0, \tag{17}$$

$$V'' = 2RU + a^2V, \tag{18}$$

$$W' = -aU, \tag{19}$$

$$T'' - a^2T = (h^2\sigma\Theta/\nu)W \equiv AW, \tag{20}$$

where σ is the Prandtl number, ν is the kinematic viscosity, $a = \beta h$ and R is the rotational Reynolds number $\Omega h^2/\nu$; the dashes denote differentiation with respect to ξ $(= z/h)$.

The boundary conditions are the same as those used in I, since they do not depend on Θ, namely

$$\left.\begin{aligned} U(0) = V(0) = W(0) = 0, \qquad T'(0) = 1, \\ U'(1) = V'(1) = W(1) = T'(1) = 0. \end{aligned}\right\} \tag{21}$$

4. Method of solution

Despite the fact that the system of differential equations (17) to (20) is a linear one, it is not practical to solve them without recourse to numerical methods. A numerical method was also employed in I but, since then, a better method for the solution of a system of linear differential equations subject to two-point boundary conditions has been described by Goodman & Lance (1956). The improved method was used for the present computations and found to be very satisfactory. The calculations were performed on a Ferranti Pegasus digital computer.

Numerical values are required for a, R and $A \equiv (h^2\sigma\Theta/\nu)$. The value of a was taken to be unity. This implies a depth of liquid of about 4 cm in a dish-pan with a radius of 15 cm. Since $\beta r_0 = 3{\cdot}83$ and $a = \beta h$, $h = r_0/3{\cdot}83$ and so, under the conditions of the experiment, for which $r_0 = 15$ cm, $\sigma \doteqdot 7$ for water at a temperature of 15° C, $\nu \doteqdot 0{\cdot}01$ and $\Theta \doteqdot 1$, it follows that $A \doteqdot 10\,737$. In the calculations the Reynolds number R was taken to be 0 (no rotation), 2, 4, 8, 16, 32 and 64.

5. Results and conclusions

Radial velocity component

Figure 1 shows the curves $U(\xi) \times 10^4$ against ξ, for $a = 1$ and $A = 10\,737$. The curves shown are for $R = 0$, 16, 32 and 64. The results for $R = 2$, 4 and 8 were computed, but they are omitted because they lie between those of $R = 0$ and $R = 16$. This figure is to be compared with figure 2*a* of I, which shows the curves when the lapse rate is zero, i.e. $A = 0$.

The following differences may be noted.

(i) In figure 1, $U \times 10^4$ is plotted, whereas in the corresponding figure of I, $U \times 10^3$ is shown. Hence, there is a considerable drop in the magnitude of the radial velocity component.

(ii) In the present case, for each value of R there is a zero of U when $\xi < 0{\cdot}5$; previously, the zero occurred when $\xi > 0{\cdot}5$.

(iii) For small R the greatest inflow $(U < 0)$ is slightly *below* the surface when $A \neq 0$, whereas when $A = 0$, the maximum inflow is *at* the surface. For large R there is a band, for which $0{\cdot}25 < \xi < 0{\cdot}75$, of comparatively slow inflow, but when $\xi > 0{\cdot}75$ the inflow increases and reaches a maximum at the surface.

(iv) In the case of $R = 64$ the radial motion tends to be concentrated in the upper and lower regions of the fluid. Such a behaviour was not apparent in the results of I.

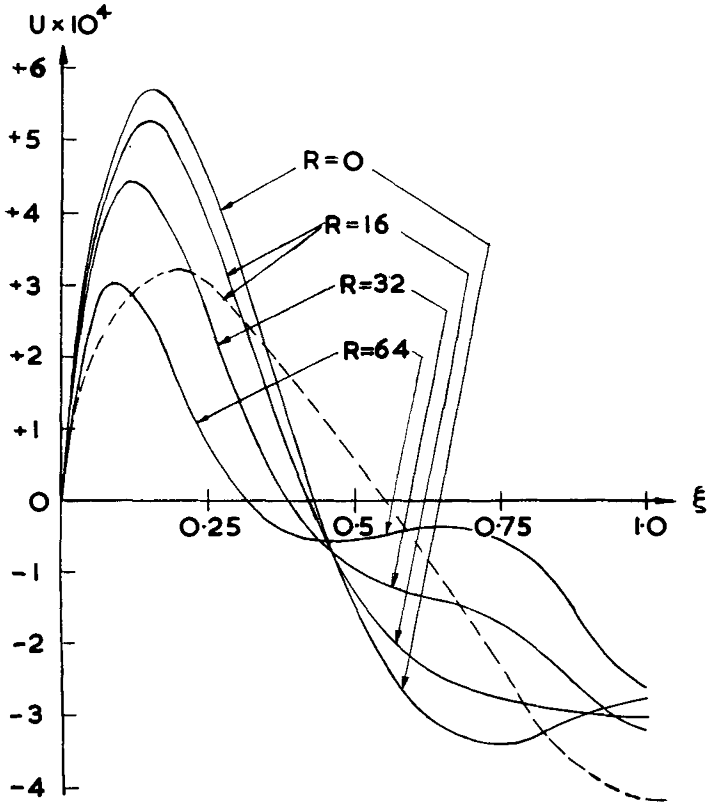

Figure 1. Non-dimensional radial velocity profile plotted against non-dimensional height. Cases for which $A = 10\,737$ are shown as solid lines. The broken curve is $A = 0$, $R = 16$ and is the value of $U \times 10^3$.

Zonal velocity component

Figure 2 shows the curves $V(\xi) \times 10^4$ against ξ, for $a = 1$ and $A = 10\,737$. The curves shown, for $R = 0$, 2, 4, 8, 16, 32 and 64, may be compared with those of figure 3 *a* in I. The following points are notable.

(i) As in the case of $U(\xi)$ there is a reduction in magnitude by a factor of 10.

(ii) The band of easterlies is confined to $\xi < 0{\cdot}2$ when $A = 10\,737$.

(iii) The maximum zonal velocity at the surface continues to increase as R increases, whereas when $A = 0$ the zonal velocity reached a maximum value when $R \doteqdot 16$. (This is only true for $R \leqslant 64$, which was the limit to which the calculations were taken.)

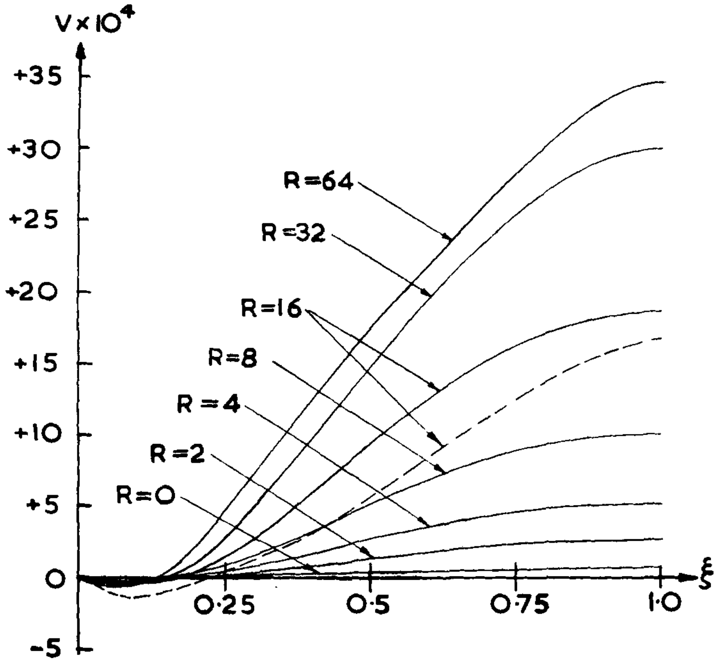

Figure 2. Non-dimensional zonal velocity profile plotted against non-dimensional height. Cases for which $A = 10\,737$ are shown as solid lines. The broken curve is $A = 0$, $R = 16$ and is the value of $V \times 10^3$.

Vertical velocity component

Figure 3 shows the curves $-W(\xi) \times 10^5$ against ξ for $a = 1$ and $A = 10\,737$. The curves for $R = 0$, 16, 32 and 64 are shown, the remainder are omitted for simplicity. The case $A = 0$ is figure 4*a* of I, and the following are the differences between the two cases.

(i) The scale factor is 10^5 in the present case as opposed to 10^3 in the case of $A = 0$.

(ii) The curve $R = 64$ shows a distinct flattening in the range $0{\cdot}25 < \xi < 0{\cdot}75$, when $A = 10\,737$, which implies that w is tending to a constant value at intermediate depths.

(iii) For each value of R the maximum vertical velocity is below $\xi = 0{\cdot}5$ when $A = 10\,737$, but when $A = 0$ the maximum is in each case above $\xi = 0{\cdot}5$.

The results, when looked at *in toto*, show that when a positive vertical lapse rate is present, the whole velocity field is reduced in magnitude. This result agrees with physical reasoning because, if the upper layers of the fluid are the warmest, then greater stability would be expected and consequently less motion.

Since the results obtained here are an order of magnitude smaller than those obtained previously it should be noted that on all the diagrams the comparison curves, which are taken from Lance & Deland, are shown dotted and are plotted to a different scale. Enough has been said in the above remarks, about the results, to make the differences apparent and the interested reader is referred to Lance & Deland for complete diagrams of the case $A = 0$.

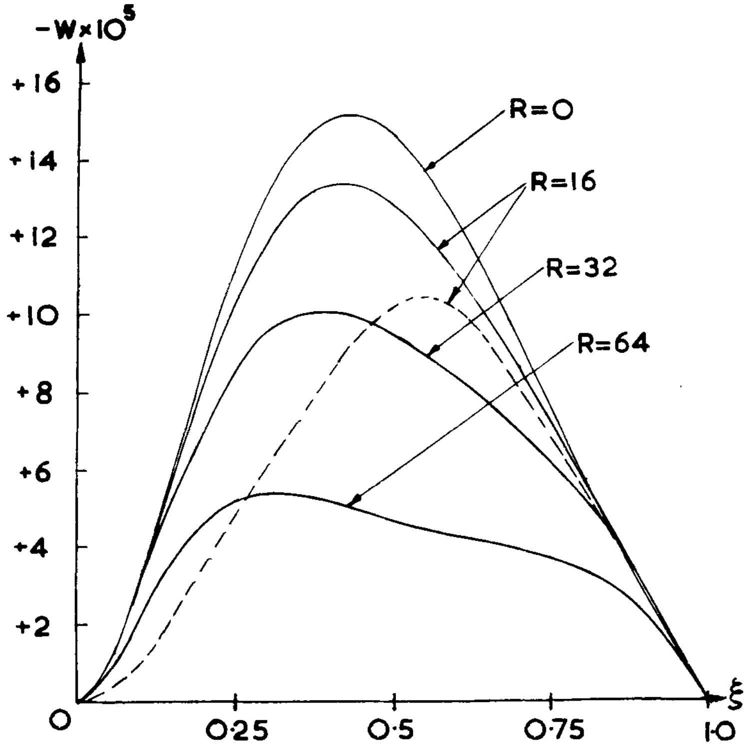

Figure 3. Non-dimensional vertical velocity profile plotted against non-dimensional height. Cases for which $A = 10\,737$ are shown as solid lines. The broken curve is $A = 0$, $R = 16$ and is the value of $-W \times 10^4$.

A detailed comparison with the experimental results of Fultz and Skeib has not been made because, in all the experiments, the value of the Reynolds number does not correspond with any of those used in the present calculations. It is obviously very desirable to extend this work to higher values of R and to other values of the depth parameter a. Such an investigation is at present in hand but it was considered worth while to publish these results as being a valuable extension of the work described in I.

The author wishes to express his thanks to Mr T. V. Davies for his valuable advice.

References

Davies, T. V. 1953 *Phil. Trans.* A, **246**, 81.

Fultz, D. 1951 Article in *Compendium of Meteorology*, p. 1235. American Meteorological Society.

Fultz, D. 1956 *Proceedings of the* 1*st Symposium on the Use of Models in Geophysical Fluid Dynamics* (Baltimore, 1953), p. 27.

Goodman, T. R. & Lance, G. N. 1956 *Math. Tab., Wash.*, **10**, 82.

Kuo, H. L. 1954 *J. Met.* **11**, 399.

Kuo, H. L. 1955 *J. Mar. Res.* **14**, 14.

Kuo, H. L. 1956 *J. Met.* **13**, 521.

Lance, G. N. & Deland, E. C. 1955 *Proceedings of the Heat Transfer and Fluid Mechanics Institute*, § 16.

Skeib, G. 1953 *Abh. Met. Hydr. Dienst.* **3**, no. 20.